



Short communication

## Time-resolved NMR metabolomics of plant cells based on a microfluidic chip



Jan Maisch<sup>a,\*</sup>, Kristina Kreppenhof<sup>b</sup>, Silke Büchler<sup>c,d</sup>, Christian Merle<sup>c,d</sup>,  
Shukhrat Sobich<sup>b</sup>, Benjamin Görling<sup>c,d</sup>, Burkhard Luy<sup>c,d</sup>, Ralf Ahrens<sup>b</sup>, Andreas E. Guber<sup>b</sup>,  
Peter Nick<sup>a</sup>

<sup>a</sup> Botanical Institute, Molecular Cell Biology, Karlsruhe Institute of Technology (KIT), Kaiserstr. 2, D-76131 Karlsruhe, Germany

<sup>b</sup> Institute of Microstructure Technology, Karlsruhe Institute of Technology (KIT), Hermann-von-Helmholtz-Platz 1, D-76344 Eggenstein-Leopoldshafen, Germany

<sup>c</sup> Institute of Organic Chemistry, Karlsruhe Institute of Technology (KIT), Fritz-Haber-Weg 6, D-76131 Karlsruhe, Germany

<sup>d</sup> Institute for Biological Interfaces, Karlsruhe Institute of Technology (KIT), Hermann-von-Helmholtz-Platz 1, D-76344 Eggenstein-Leopoldshafen, Germany

### ARTICLE INFO

#### Article history:

Received 23 February 2016

Received in revised form 2 June 2016

Accepted 2 June 2016

Available online 10 June 2016

#### Keywords:

Microfluidics

NMR metabolomics

Tobacco cells (*Nicotiana tabacum* L. cv. BY-2)

### ABSTRACT

The plant secondary metabolism generates numerous compounds harbouring pharmaceutical activity. In plants, these compounds are typically formed by different and specialised cell types that have to interact constituting a metabolic process chain. This interactivity impedes biotechnological production of secondary compounds, because cell differentiation is suppressed under the conditions of a batch bioreactor. We present a novel strategy to address this limitation using a biomimetic approach, where we simulate the situation in a real tissue by a microfluidic chamber system, where plant cells can be integrated into a process flow. We show that walled cells of the plant model tobacco BY-2 can be successfully cultivated in this system and that physiological parameters (such as cell viability, mitotic index and division synchrony) can be preserved over several days. The microfluidic design allows to resolve dynamic changes of specific metabolites over different stages of culture development. These results serve as proof-of-principle that a microfluidic organisation of cultivated plant cells can mimic the metabolic flows in a real plant tissue.

© 2016 Elsevier GmbH. All rights reserved.

### 1. Introduction

Plants not only represent the primary food source on this planet, but also produce a large number of secondary compounds (according to current estimates  $\sim 10^6$ ; Saito and Matsuda, 2010). These compounds provide the molecular base for the traditional use of plants for medicine or as aromatic flavours. Many of these, often valuable and costly, compounds cannot be synthesised *in vitro*, such that they have to be extracted from their natural source. The complex metabolic pathways yielding these compounds usually require the cooperation of several cell types, transport between different tissues, and the accumulation in specific, often individual secretion cells, rendering extraction from the natural source expensive and inefficient. In addition, many of these plants are endangered and under strong pressure by non-sustainable human exploitation.

In situations, where small amounts of costly products have to be produced, plant molecular farming as relatively new branch of green gene technology is superior to transgenic animals or transgenic microorganisms (Daniell et al., 2003). Since molecular farming is performed in closed systems, typically fermenters or cell cultures, release of genetically modified organisms into the environment, a topic raising public concern, at least in Europe, can be circumvented. However, a closer look shows that this approach has been successful almost exclusively for peptide- or protein-based pharmaceutically active compounds. The wealth of plant secondary metabolism still remains to be exploited. This is not due to a lack of interest: The synthesis of the precious anti-cancer drug vinblastine in cell cultures of *Catharanthus roseus* has been pursued for almost half a century without significant success (Rischer et al., 2006).

A possible reason for this difficulty might be the fact that secondary metabolism is not only strictly assigned to different compartments within the producer cell, but, in addition, has to be subdivided between cells of different types. Thus, secondary plant metabolism is characterised by dynamic changes of metabolic fluxes conveyed from one cell type to the next. This can neither be studied nor technically achieved by batch-fermenter systems.

\* Corresponding author.

E-mail address: [Jan.Maisch@kit.edu](mailto:Jan.Maisch@kit.edu) (J. Maisch).

To circumvent these drawbacks, we have adopted a microfluidic approach, where small numbers of cells of the different cell types are cultivated in individual cell chambers which are interconnected by a common transfer channel system. The upper cell compartments and the lower transfer channel system are separated by a porous membrane, allowing the exchange of plant nutrient and metabolic products by diffusion. This design allows to couple different cell types into a metabolic flow to mimic the process chain in a real plant. Moreover, it is principally possible to combine different proportions of different cell types to modulate the metabolic stream, or to adjust stoichiometries.

Despite extensive research on animal cells the application of microfluidics for plant cells studies has not been accomplished yet (Sanati Nezhad, 2014). Although microfluidic devices have been used to study different aspects of plant cell biology such as gene expression (Busch et al., 2012), cell biomechanics (Sanati Nezhad et al., 2013a,b), cellular mechanism of growth (Agudelo et al., 2013; Grossmann et al., 2011; Sanati Nezhad et al., 2014), phenotyping of plant organs (Jiang et al., 2014), and chemical stimulation of plant cells (Sanati Nezhad et al., 2013c), they had not been performed adequately enough with walled plant cells, so far. The reason is that these cells are not attached to a surface as mammalian cells, but have to be cultivated in suspension. To our knowledge, only two reports have been published, where plant cells were cultivated in a microfluidic chip (Ko et al., 2006; Wu et al., 2011). However, these were protoplasts, where the cell wall was removed and therefore highly distorted in their physiology. Our work is the first demonstrating cultivation of walled plant cells in a microfluidic chip which is able to preserve the physiology of these cells over time.

To demonstrate the feasibility of our strategy, metabolites in the flow-through have to be monitored in a time-resolved manner. For this purpose, we employed NMR spectroscopy. This analytical method allows the simultaneous detection of all proton-containing compounds in a single analytical run (Luy, 2011). The measurement is inherently quantitative and unbiased, and thus suited to detect even subtle changes as well as the discovery of novel molecules. In addition, NMR is contact-free and non-destructive, such that the analysis will not compromise yield or integrity of the desired product. By the virtue of these advantages, NMR metabolomics has developed into a central strategy to characterise extracts from medical plants (Holmes et al., 2006).

In addition to the analytical method, the choice of the cellular model is important. We decided to use tobacco BY-2 suspension cells, a central model system in plant cell biology (Opatrný et al., 2014). As a member of the chemically proficient family of Solanaceae, tobacco is endowed with a rich secondary metabolism, giving rise to numerous alkaloids with pharmacological activity. The BY-2 cell strain can be readily transformed, a prerequisite for efficient metabolic engineering. The cell biology and the physiological parameters of this cell strain have been thoroughly characterised, such that the behaviour of these cells in the microfluidic environment can be monitored and interpreted with great precision.

In the current work we present a novel microfluidic chamber system for plant cells and demonstrate that the BY-2 plant cell system can be successfully integrated into this system while preserving features of their physiology. As third component, NMR spectroscopy as a non-invasive analytical strategy, is integrated to demonstrate time-resolved changes of metabolic activity.

## 2. Materials and methods

### 2.1. Fabrication of the microfluidic chip

For the fabrication of the microfluidic chip hot embossing (Worgull, 2009) was chosen as strategy. This technique allows

**Table 1**  
Temporal organisation of the cultivation experiments.

Experiment	Loading: cell age [d]	Time in chamber [h]	Extraction: cell age [d]
I	0	96	4
II	2	72	5
III	3	96	7
Cell suspension controls			4, 5, 7

to replicate the microfluidic components from a mold insert, using different types of polymers. However, first prototypes have been produced by direct micromilling of appropriate polycarbonate plates. For hot embossing, the components were generated from polycarbonate (Makrofol® DE 1-1, Bayer Material Science AG, Leverkusen, Germany) from a brass mold-insert, fabricated by micromachining (i-sys Mikro- und Feinwerktechnik GmbH, Karlsruhe, Germany) according to the design given in Fig. 1. Subsequently, the upper and lower compartments, and an ion track-etched polycarbonate membrane (Isopore™ membrane filter with 0.4 μm pore diameter, EMD Millipore Corporation, Billerica, USA) were sealed liquid-tight by thermal bonding (Becker and Gärtner, 2008; Tsao and DeVoe, 2009).

### 2.2. Operation of the microfluidic chip

The microfluidic chip as shown in Fig. 1 was first perfused with 70% (v/v) ethanol to exclude contaminations, and then filled with sterile liquid medium. A constant flow of 77 μL/min within the lower compartment was adjusted using a peristaltic pump (Ismatec Reglo Digital MS-CA4/12-100, Ismatec, Wertheim, Germany). Tobacco suspension cells of different age (0 d,  $5 \times 10^4$  cells/mL; 2 d,  $3 \times 10^5$  cells/mL; 3 d;  $8.5 \times 10^5$  cells/mL) were injected into the upper compartment and further cultivated for 72–96 h at 26 °C as shown in Table 1. Starting with day 1 of cultivation, 770 μL of the flow through were harvested from the lower chamber and analysed by NMR every hour for 5–8 h during work day. The cells were extracted from the upper compartment after 72 or 96 h of cultivation and analysed as described below (Table 1).

### 2.3. Tobacco cell culture

BY-2 (*Nicotiana tabacum* L. cv Bright Yellow 2) suspension cells (Nagata et al., 1992) were cultivated in liquid medium containing 4.3 g L<sup>-1</sup> Murashige and Skoog salts (Duchefa, Haarlem, The Netherlands), 30 g L<sup>-1</sup> sucrose, 200 mg L<sup>-1</sup> KH<sub>2</sub>PO<sub>4</sub>, 100 mg L<sup>-1</sup> inositol, 1 mg L<sup>-1</sup> thiamine, and 0.2 mg L<sup>-1</sup> (0.9 μM) 2,4-D, pH 5.8. The cells were subcultivated weekly, inoculating 1.0–1.5 mL of stationary cells into fresh medium (30 mL) in 100-mL Erlenmeyer flasks. The cells were incubated at 26 °C under constant shaking on a KS260 basic orbital shaker (IKA Labor Technik, Staufen, Germany) at 150 rpm. Every three weeks the stock BY-2 calli were subcultured on media solidified with 0.8% (w/v) agar (Roth, Karlsruhe, Germany).

### 2.4. Phenotyping of cellular physiology

Viability of the cells was followed over cultivation time in the microchamber using an assay based on the Evans Blue dye exclusion test (Gaff and Okong'O-Ogola, 1971). Living cells possess intact cell membranes that exclude the Evans Blue dye, whereas dead cells do not. To detect potential effects of chamber cultivation on the proliferation status of the cells, the mitotic index was measured, as previously described (Maisch and Nick, 2007). The mitotic index gives the proportion of cells in prophase, metaphase, anaphase and telophase. To discriminate non-mitotic (uncondensed chromatin)

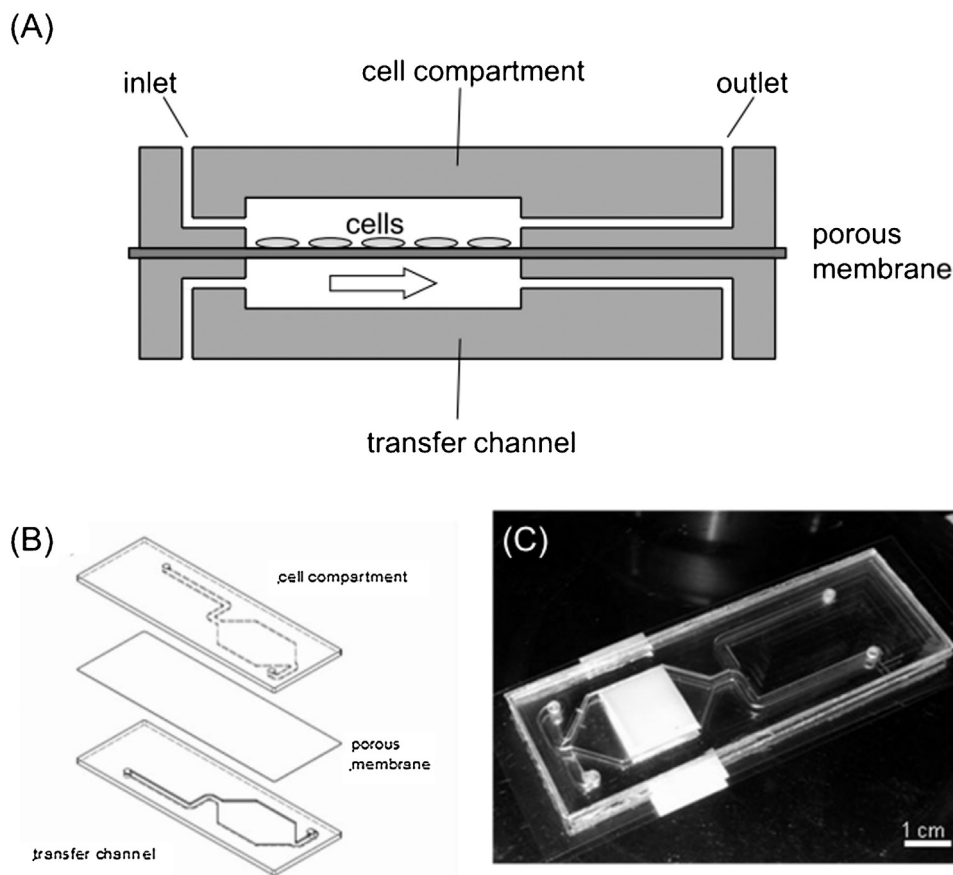


**Fig. 1.** Design and function of the microfluidic chip. (A) Schematic representation of the microfluidic chip with a cell compartment in the upper layer and a corresponding transfer channel in the lower layer. After the cell compartment has been filled with the cells, inlet and outlet are closed while the transfer channel is operated continuously. The arrow indicates the constant flow of medium. (B) Exploded view of the microfluidic chip (C) Photograph of the microfluidic chip where the white band indicates the porous area of the membrane.

from mitotic (condensed chromosomes) cells, the fluorescent dye Hoechst 22358 (Sigma-Aldrich, Neu-Ulm, Germany) intercalating into the DNA was used. Cell division synchrony monitors the polar transport of auxin through the cell file and so far represents the most sensitive indicator for impaired actin function (Maisch and Nick, 2007). To quantify division synchrony, frequency distributions over the number of cells per individual file were constructed using an AxioImager microscope (Zeiss, Jena, Germany) equipped with a CCD (Axio-Cam MRm, Zeiss) digital imaging system and differential interference contrast. Images were acquired by the AxioVision 4.7 software (Zeiss). For detection of mitotic cells, samples were observed using the filter set 49 (excitation at 365 nm, beamsplitter at 395 nm, and emission at 445 nm). Each data point represents 3000 cells (cell viability, mitotic index) or cell files (division synchrony) from three independent experimental series. The results were tested for significance by a Student's *t*-test at the 97% confidence level. Error bars indicate standard error of the mean (SEM).

### 2.5. NMR-analysis

Aliquots of the flow-through were collected at different time points under sterile conditions. The obtained samples were shock-frozen in liquid nitrogen and stored at  $-80^{\circ}\text{C}$  till analysis. For sample preparation, the frozen aliquots were thawed for one hour at room temperature. After addition of 720  $\mu\text{L}$  culture medium, 80  $\mu\text{L}$   $\text{D}_2\text{O}$ , and 580  $\mu\text{M}$  TSP (perdeuterated

3-(trimethylsilyl)propionic acid sodium salt), the sample was vigorously mixed for 1 min, and 600  $\mu\text{L}$  of the mixture was transferred into 5-mm Duran<sup>®</sup> Standard NMR tubes (Schott, Mainz; Germany) for analysis. For each sample, one-dimensional (1D)  $^1\text{H}$ -excited and  $^1\text{H}$ -detected standard presaturated nuclear Overhauser enhancement spectroscopy (NOESY) spectra were measured at 599.87 MHz resonance frequency on a Bruker Avance III 600 MHz spectrometer (Bruker Corporation, Billerica, USA). 65536 data points were acquired corresponding to an acquisition time of 2.66 s. The pulse sequence designed for automated water suppression and reliable integration of metabolite signals was used as provided by the standard Bruker pulse programme library. The 1D spectra were recorded with 32 scans and 4 dummy scans with a receiver gain of 90.5. Presaturation was set to 4 s with an rf-amplitude corresponding to a  $90^{\circ}$   $^1\text{H}$  hard pulse of 10 ms (25 Hz) and the mixing delay was chosen to 10 ms. All spectra were processed with zero filling up to 65536 points without any apodisation. The baseline-separated signals were integrated by selecting the signals of the corresponding compound manually. For quantifications shown in Fig. 3, the obtained peak areas for isolated signals of glucose from 5.25 ppm to 5.22 ppm, and for myo-inositol myo-inositol from 3.29 to 3.28 ppm were calibrated relative to the TSP reference signal. Integrated intensities of sucrose do not show any correlation with either glucose or fructose, so that an enzymatic degradation of sucrose to its monosaccharides can be excluded as the main source of the observed time dependence of glucose concentrations in the medium.

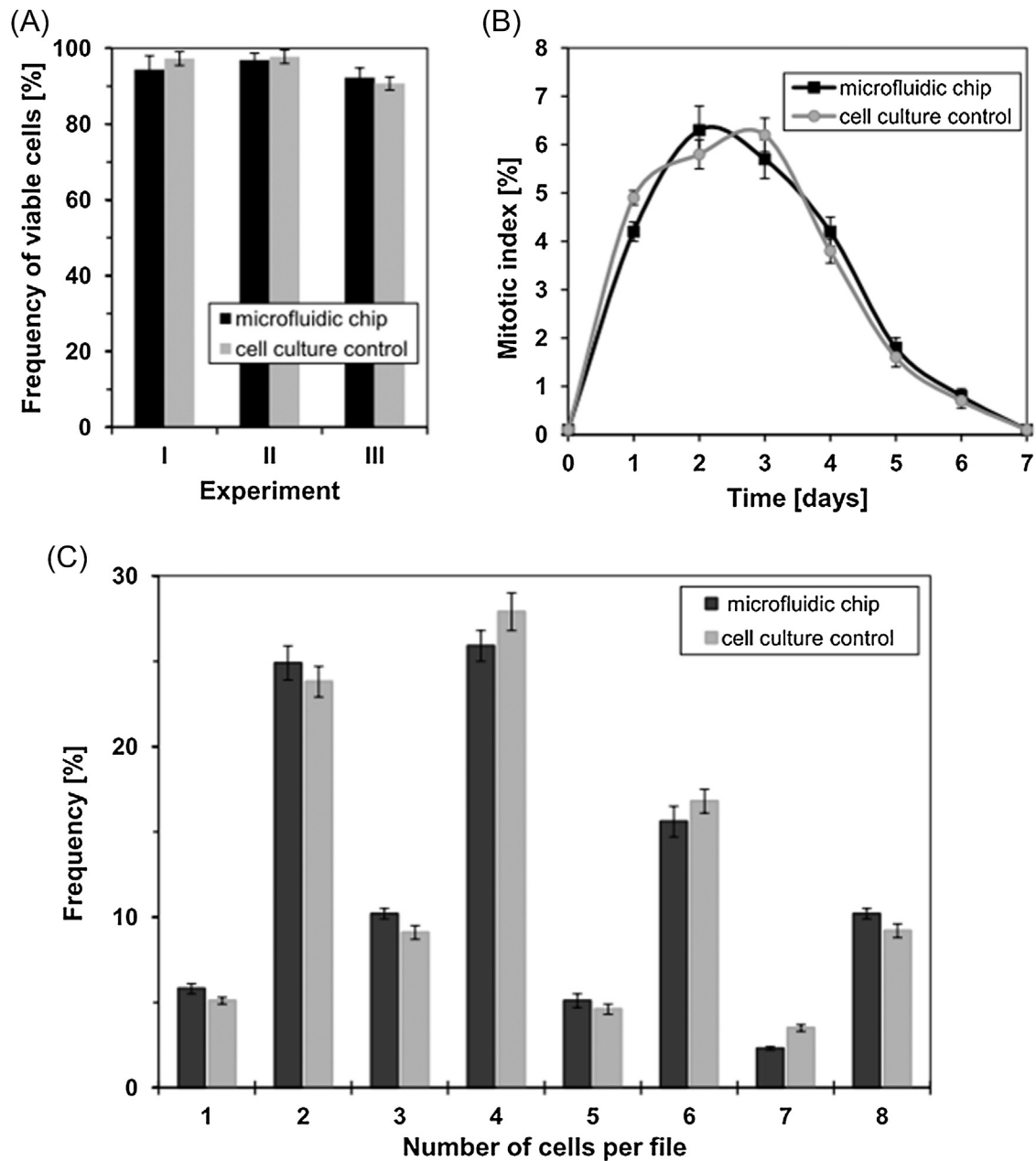


**Fig. 2.** Phenotypic parameters of tobacco BY-2 cells upon cultivation in microfluidic chips of the design shown in Fig. 1 (black) as compared to conventional cultivation in suspension (grey). (A) Cell viability assayed at day 4 (Experiment I), day 5 (Experiment II), and day 7 (Experiment III) by the Evans Blue dye exclusion test. (B) Mitotic indices over time. (C) Division synchrony measured as frequency distribution over cell number per file. Each data point represents 3000 cells (cell viability, mitotic index) or cell files (division synchrony) from three independent experimental series. Error bars indicate standard error of the mean (SEM).

### 3. Results

#### 3.1. Design of the chip

For the setup of the microfluidic chip we used hot-embossed components of a microfluidic chip which was previously described (Kim et al., 2012). For this application two identical parts with large compartments have been assembled as shown in Fig. 1. Both compartments are separated by a porous membrane. The upper compartment is used for the cultivation of the cells (cell compartment). In the lower compartment (transfer channel) a constant flow of culture medium is applied. The chip represents one module which can be connected to other modules using appropriate tubing. The outer dimensions of the chip correspond to that of a microscope slide (26 mm × 76 mm). Due to the requirements of the

previous application (Kim et al., 2012) only one half of the area is used for the cell compartment, which has the shape of an elongated hexagon to reduce problems with remaining air bubbles after filling the structures with a fluid. The 15 mm wide cell compartment has a length of about 28 mm and a height of 0.4 mm, resulting in a volume of about 132  $\mu\text{L}$ . The width of 2 mm of the fluidic channels which have the same height as the compartments was mainly chosen for better access at the fluidic ports.

#### 3.2. The microfluidic chip preserves the physiology of tobacco BY-2 cells

To test, whether the physiology of the tobacco BY-2 cells is affected during the cultivation in the microfluidic chip, we ana-

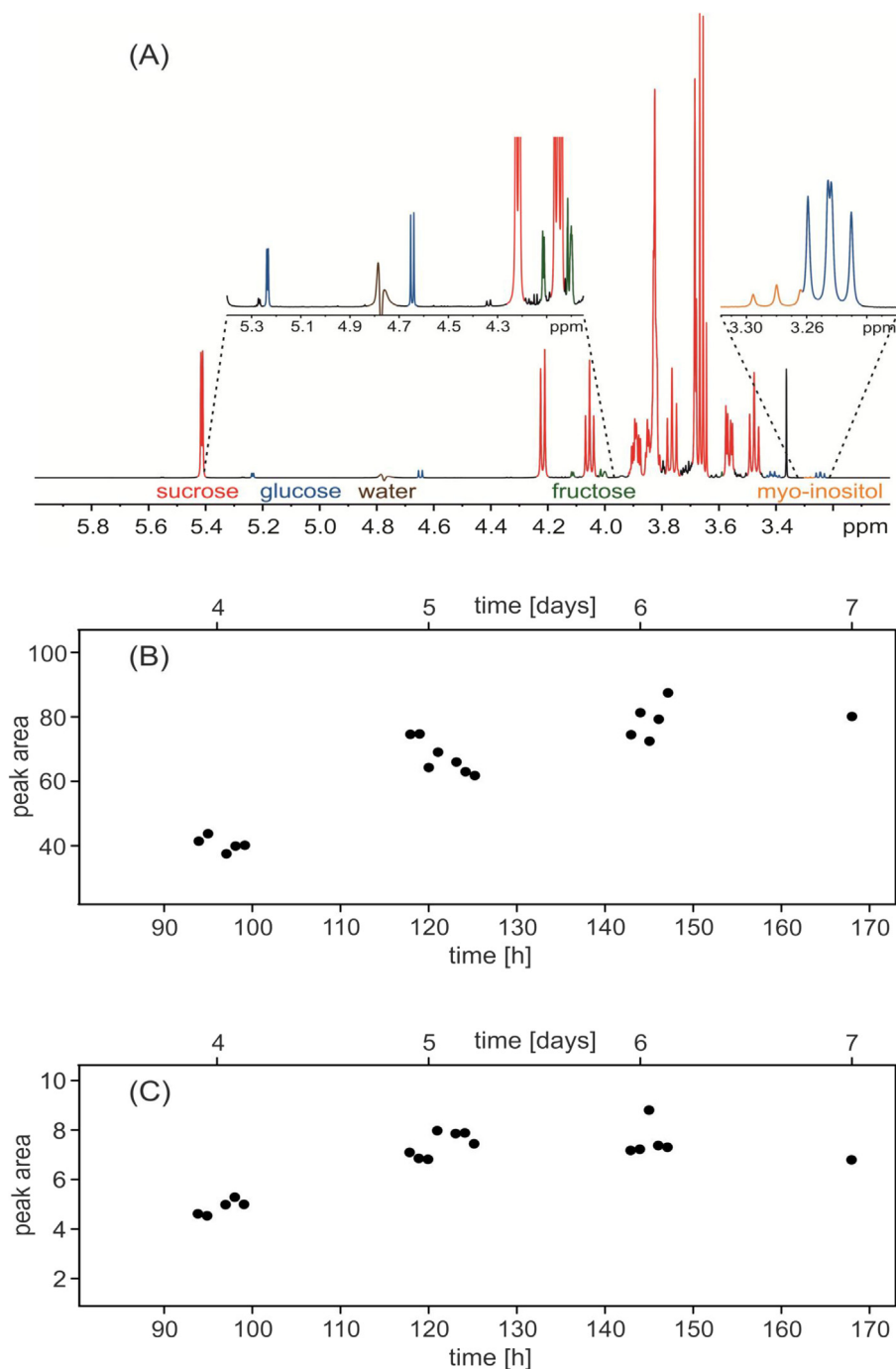


**Fig. 3.** Changes of metabolic activity followed over time by NMR spectroscopy. (A) Central region of a 1D <sup>1</sup>H presaturated NOESY spectrum. The coloured NMR peaks are unambiguously assigned to compounds in the medium. The highlighted lines indicate the signals of sucrose (red), glucose (blue), fructose (green) and myo-inositol (orange). The water signal (brown) was suppressed by a 4 s presaturation delay to a residual background signal. Time-peak area-diagrams show the time response of the substances after their passage through the microfluidic device with living BY-2 cells. Samples were taken at several hourly time-points during days 4–7. Time courses of abundance in the flow-through are shown for glucose monitoring primary catabolism (B), and myo-inositol monitoring cell-division related signalling (C) (For interpretation of the references to colour in this figure legend, the reader is referred to the web version of this article.).

lysed cell physiological parameters such as cell viability, mitotic index and division synchrony.

Viability of the cells cultivated in the microfluidic chip exceeded 95% irrespective of cultivation time and age and thus equalled the viability of cells grown conventionally in suspension (Fig. 2A, Fig. S1). Since a cell may remain viable, although it is affected in proliferation, we measured the mitotic index over time (Fig. 2B). Again, the division rate of the cells in the microfluidic chips did not exhibit any significant differences to that measured for control cells cultivated in suspension. Even the temporal sequence of division activity with

a characteristic peak at days 2–3 and a subsequent drop of proliferation, when cells enter their expansion phase, were preserved. Maximal proliferation reached around 6% in both cases. Since the central parameters were not altered by the cultivation in the chip, we asked, whether further aspects of physiology were preserved as well. Cell division synchrony monitors the polar transport of auxin through the cell file and so far represents the most sensitive indicator for intercellular communication. Even for this highly sensitive parameter that monitors self organisation by a polar auxin flow through the cell file, we could not observe any differences between

the two cultivation regimes (Fig. 2C). The characteristic peaks of frequency for cell files composed of two (25%), four (27%) and six cells (16%) observed at day 4 of cultivation were detectable at equal amplitudes in both experimental approaches.

Thus, the results from this study clearly show that the cells cultivated in microfluidic chips are viable over a long time period, that they divide and grow normally, and that their physiology is preserved during cultivation in the microchamber.

### 3.3. NMR can resolve metabolic activity in time

NMR spectroscopy was used to follow changes of metabolic activity over time. As shown representatively for a standard NOESY-presat 1D  $^1\text{H}$  spectrum of the flow-through, different metabolites can be identified by annotation of their specific signatures (Fig. 3A, Fig. S2). Numerous signals are visible with a high dynamic range of 10000 that allows the simultaneous detection of compounds with concentrations ranging from approximately 10  $\mu\text{M}$  to 100 mM. This means that changes in the level of growth regulators or specific secondary compounds (typically in the range of 1–50  $\mu\text{M}$ ) can be followed as well as modulations of primary metabolism (typically in the range of 10–100 mM). Assignment of peaks to the corresponding metabolites shown here has been achieved by both comparison with databases and sample spiking for the respective compound.

To test the feasibility of this approach, changes in the abundance of two example metabolites, glucose as readout for primary metabolism (Fig. 3B), and *myo*-inositol as readout for signalling (Fig. 3C) were followed over the time of cultivation (as quantified by the integrated area of the respective peaks).

The medium contains sucrose as energy source for the heterotrophic BY-2 cells. After autoclaving of the whole batch of the medium, sucrose is partly converted into glucose and fructose. Up to day 4, the level of glucose detected in the flow-through is relatively low, reflecting the strong consumption of energy during the intensive proliferation phase (compare Fig. 2B). Between day 4 and 5, the relative abundance of glucose increases by a factor of 2 and remains high till the end of the culture cycle correlating with a concomitant sharp decrease of mitotic activity (Fig. 2B). A likely interpretation of this pattern is that the reduction of catabolic activity after completion of the proliferation phase reduces the uptake of glucose in the medium.

The detection of *myo*-inositol in the flow-through (Fig. 3C) shows a similar temporal pattern, however, at an abundance that is around tenfold lower as compared to glucose. Low concentrations of *myo*-inositol (for the Murashige–Skoog medium used in the current experiments, the concentration is 100  $\text{mg L}^{-1}$ ) are added to most culture media as supplement. Unlike sucrose, *myo*-inositol is not required as energy source, but as precursor for different inositol phosphates, important signalling components that are required to convey the signal generated through the activation of a trimeric G-protein by the artificial auxin 2,4-D towards the machinery that activates cell division (Campanoni and Nick, 2005). From this function it can be predicted that *myo*-inositol should be consumed up to day 4 such that its abundance in the flow-through is expected to be low. Upon completion of proliferation, the activity of the trimeric G-protein is expected to decrease, such that *myo*-inositol is no longer required and therefore should remain in the flow-through leading to an increased signal. Our observations (Fig. 3C) are congruent with this prediction.

## 4. Discussion

As novel approach towards biotechnological production of pharmacologically interesting plant secondary compounds, we have

designed for the first time a microfluidic chamber system which allows to cultivate walled plant cells of interest and to harvest their products in the flow-through. As proof of principle we have successfully integrated the plant model tobacco BY-2 into this chamber system. We demonstrate here that the cells can be kept viable over an entire cultivation cycle. Moreover, we can show that their proliferation activity is preserved as well as details of their physiology and self organisation, such as cell division synchrony (see Fig. 2). By NMR spectroscopy we can resolve dynamic changes of specific metabolites in the flow-through of this system and we can assign these to specific cellular processes such as mitotic activity.

We have used NMR analytics to explore the potential of a future real-time metabolic consumption analysis, which would be possible through this non-invasive technique. We have selected two examples (glucose as abundant, *myo*-inositol as non-abundant molecule) to test the potential of the technique. These two representative examples demonstrate that dynamic changes in the chemical composition of the flow-through can be used to monitor developmental changes of metabolic activity in the microfluidic chip (Fig. 3). In the conventional batch culture, so far, it has only been possible to measure the integrals of metabolic changes and it was not possible to link it with particular developmental stages.

These results not only serve as proof-of-principle that a microfluidic organisation of cultivated plant cells can mimic the metabolic flows in a real plant tissue, but also clearly demonstrate that the microfluidic device allows insight into the dynamics of metabolism generating experimental models that would not be accessible by conventional cultivation of plant cells.

In the future, our approach can be expanded by combination of different chambers harbouring cells differing in their metabolic status (either in consequence of specific pretreatments, specific source tissues, or genetic engineering). By changing the analytical approach to flow-NMR instruments, it should become possible to integrate medium-based monitoring in real time that might be used to adjust influx of substrates or medium depending on feedback from the envisaged product in the flow-through.

### Conflict of interest

The authors declare that they have no conflict of interest.

### Funding

The authors declare no competing financial interests.

### Author contributions

J.M., B.G., B.L., R.A., A.E.G., and P.N. designed the experiments and wrote the manuscript. J.M., K.K., S.B., C.M., and S.S. performed the experiments. All authors have read and approved the final manuscript.

### Acknowledgements

B.L. thanks the HGF BioInterfaces programme and the Fonds der Chemischen Industrie for financial support. NMR spectra were acquired at the Pro<sup>2</sup>NMR instrumentation facility. This work was partly carried out with the support of the Karlsruhe Nano Micro Facility (KNMF, [www.kit.edu/knmf](http://www.kit.edu/knmf)), a Helmholtz Research Infrastructure at Karlsruhe Institute of Technology.

### Appendix A. Supplementary data

Supplementary data associated with this article can be found, in the online version, at <http://dx.doi.org/10.1016/j.jplph.2016.06.004>.

## References

- Agudelo, C.G., Sanati Nezhad, A., Ghanbari, M., Naghavi, M., Packirisamy, M., Geitmann, A., 2013. *Plant J.* **73**, 1057–1068.
- Becker, H., Gärtner, C., 2008. *Anal. Bioanal. Chem.* **390**, 89–111.
- Busch, W., Moore, B.T., Martsberger, B., Mace, D.L., Twigg, R.W., Jung, J., et al., 2012. *Nat. Methods* **9**, 1101–1106.
- Campanoni, P., Nick, P., 2005. *Plant Physiol.* **137**, 939–948.
- Daniell, H., Streatfield, S.J., Wycoff, K., 2003. *Trends Plant Sci.* **6**, 219–226.
- Gaff, D.F., Okong'O-Ogola, O., 1971. *J. Exp. Bot.* **22**, 756–758.
- Grossmann, G., Guo, W.-J., Ehrhardt, D.W., Frommer, W.B., Sit, R.V., Quake, S.R., Meier, M., 2011. *Plant Cell* **23**, 4234–4240.
- Holmes, E., Tang, H., Wang, Y., Seger, C., 2006. *Planta Med.* **72**, 771–785.
- Jiang, H., Xu, Z., Aluru, M.R., Dong, L., 2014. *Lab Chip* **14**, 1281–1293.
- Kim, C., Kreppenhof, K., Kashef, J., Gradi, D., Herrmann, D., Schneider, M., et al., 2012. *Lab Chip* **12**, 5186–5194.
- Ko, J.-M., Ju, J., Lee, S.H., Cha, H.-C., 2006. *Protoplasma* **227**, 237–240.
- Luy, B., 2011. *Angew. Chem. Int.* **50**, 354–356.
- Maisch, J., Nick, P., 2007. *Plant Physiol.* **143**, 1695–1704.
- Nagata, T., Nemoto, Y., Hasezawa, S., 1992. *Int. Rev. Cytol.* **132**, 1–30.
- Opatrný, Z., Nick, P., Petrášek, J., 2014. *Applied Plant Cell Biology*. In: Opatrný, Z., Nick, P. (Eds.). Springer, Heidelberg, pp. 455–481.
- Rischer, H., Orešič, M., Seppänen-Laakso, T., Katajamaa, M., Lammertyn, F., Ardiles-Diaz, W., et al., 2006. *Proc. Natl. Acad. Sci. U. S. A.* **103**, 5614–5619.
- Saito, K., Matsuda, F., 2010. *Annu. Rev. Plant Biol.* **61**, 463–489.
- Sanati Nezhad, A., Naghavi, M., Packirisamy, M., Bhat, R., Geitmann, A., 2013a. *Lab Chip* **13**, 2599–2608.
- Sanati Nezhad, A., Naghavi, M., Packirisamy, M., Bhat, R., Geitmann, A., 2013b. *Proc. Natl. Acad. Sci. U. S. A.* **110**, 8093–8098.
- Sanati Nezhad, A., Packirisamy, M., Bhat, R.B., Geitmann, A., 2013c. *Biomed. Eng.* **60**, 3185–3193.
- Sanati Nezhad, A., Ghanbari, M., Agudelo, C.G., Naghavi, M., Packirisamy, M., Bhat, R.B., et al., 2014. *Biomed. Microdevices* **16**, 22–33.
- Sanati Nezhad, A., 2014. *Lab Chip* **14**, 3262–3274.
- Tsao, C.W., DeVoe, D.L., 2009. *Microfluid. Nanofluid.* **6**, 1–16.
- Worgull, M., 2009. *Micro & Nano Technologies*. In: Ramsden, J.J. (Ed.). Elsevier, Oxford.
- Wu, H., Liu, W., Tu, Q., Song, N., Li, L., Wang, J., Wang, J., 2011. *Microfluid. Nanofluid.* **10**, 867–876.